Montes Christian (Orcid ID: 0000-0003-1249-2308) Walley Justin (Orcid ID: 0000-0001-7553-2237)

Integration of multi-omics data reveals interplay between brassinosteroid and TORC signaling in Arabidopsis

Christian Montes¹, Ping Wang², Ching-Yi Liao², Trevor M Nolan^{2,3}, Gaoyuan Song¹, Natalie M Clark¹, J. Mitch Elmore^{1,4}, Hongqing Guo², Diane C Bassham², Yanhai Yin^{2,5}, Justin W Walley^{1,5*}

¹Department of Plant Pathology and Microbiology, lowa State University, Ames, IA 50011, USA; ²Department of Genetics, Development and Cell Biology, lowa State University, Ames, IA 50011, USA; ³Department of Biology, Duke University, Durham, NC 27708, USA; ⁴USDA-ARS Cereal Disease Laboratory, University of Minnesota, St. Paul, MN 55108, USA; ⁵Plant Sciences Institute, lowa State University, Ames, IA 50011, USA * Corresponding Author: Justin Walley (jwalley@iastate.edu)

Received: 6 April 2022 Accepted: 16 July 2022

ORCID:

Christian Montes: 0000-0003-1249-2308

Ping Wang: 0000-0002-4484-6329

Ching-Yi Liao: 0000-0002-5050-2995

Trevor M Nolan: 0000-0003-1362-2557

Gaoyuan Song

Natalie M Clark: 0000-0003-0988-321X

J. Mitch Elmore

Hongqing Guo: 0000-0003-1498-3733

Diane C Bassham: 0000-0001-7411-9360

Yanhai Yin

Justin W Walley: 0000-0001-7553-2237

This article has been accepted for publication and undergone full peer review but has not been through the copyediting, typesetting, pagination and proofreading process which may lead to differences between this version and the Version of Record. Please cite this article as doi: 10.1111/nph.18404

Summary

- Brassinosteroids (BR) and Target of Rapamycin Complex (TORC) are two major actors coordinating plant growth and stress responses. BRs function through a signaling pathway to extensively regulate gene expression and TORC is known to regulate translation and autophagy. Recent studies have revealed connections between these two pathways, but a system-wide view of their interplay is still missing.
- We quantified the level of 23,975 transcripts, 11,183 proteins, and 27,887 phosphorylation sites in wild-type *Arabidopsis thaliana* and in mutants with altered levels of either BRASSINOSTEROID INSENSITIVE 2 (BIN2) or REGULATORY ASSOCIATED PROTEIN OF TOR 1B (RAPTOR1B), two key players in BR and TORC signaling, respectively.
- We found that perturbation of BIN2 or RAPTOR1B levels affects a common set of gene-products involved in growth and stress responses. Furthermore, we used the multi-omic data to reconstruct an integrated signaling network. We screened 41 candidate genes identified from the reconstructed network and found that loss of function mutants of many of these proteins led to an altered BR response and/or modulated autophagy activity.
- Altogether, these results establish a predictive network that defines different layers
 of molecular interactions between BR- or TORC-regulated growth and autophagy.

Key words: Autophagy, BIN2, Brassinosteroids, integrative, multi-omics, network, RAPTOR, TOR.

Introduction

Organisms are frequently affected by environmental challenges. When responding to stress, specific molecular and cellular processes are triggered, and growth is often compromised. These responses to both biotic and abiotic stresses rely heavily on modulating hormonal signaling pathways, and plants need to allocate resources between their growth and stress response machinery efficiently. Therefore, well-coordinated hormonal crosstalk is fundamental for a successful response to stress (Huot *et al.*, 2014; Verma *et al.*, 2016; Bürger & Chory, 2019). The growth-promoting hormone brassinosteroid (BR) has been shown as a critical element in this balance. Plants with altered levels of BR signaling or biosynthesis genes exhibit deficient growth (Li *et al.*, 1996; Li & Chory, 1997; Li & Nam, 2002; Yin *et al.*, 2002; Chung *et al.*, 2010; Guo *et al.*, 2013) and abnormal response to various stresses (Che *et al.*, 2010; Ye *et al.*, 2017; Nolan *et al.*, 2017a; Gruszka, 2018; Fàbregas *et al.*, 2018; Planas-Riverola *et al.*, 2019; Xie *et al.*, 2019; Gupta *et al.*, 2020; Liang *et al.*, 2020).

The GLYCOGEN SYNTHASE KINASE 3 (GSK3)-like kinase BRASSINOSTEROID INSENSITIVE 2 (BIN2) is a critical negative regulator of BR signaling (Li & Nam, 2002; Kim et al., 2009). In the absence of BRs, BIN2 phosphorylates the bri1-EMS-SUPPRESSOR1/BRASSINAZOLE RESISTANT1 (BES1/BZR1) family of transcription factors (TFs), which reduces their protein level, lowers DNA binding, and promotes cytoplasmic sequestration by 14-3-3 proteins, thereby preventing the activation of downstream BR response genes (Yin et al., 2002; Gampala et al., 2007; Ryu et al., 2007, 2010). BR signals through the receptor BRI1, coreceptor BAK1, and other components to inhibit BIN2, allowing BES1/BZR1 accumulation in the nucleus to regulate thousands of BR genes for various BR responses (Li & Chory, 1997; Wang et al., 2001; Nam & Li, 2002; Kim et al., 2009; Zhu et al., 2017; Nolan et al., 2020). Besides regulating BES1 and BZR1, increasing evidence position BIN2 as a hub for regulation of the balance between stress and growth (Youn & Kim, 2015; Nolan et al., 2020). BIN2 is involved in BRregulation of diverse processes such as drought and abscisic acid (ABA) signaling (Cai et al., 2014; Hu & Yu, 2014; Ye et al., 2017; Jiang et al., 2019), cold stress response (Ye et al., 2019), salt-stress response (Li et al., 2020b), root development in conjunction with auxin signaling (Cho *et al.*, 2014; Li *et al.*, 2020a) as well as chloroplast development (Zhang *et al.*, 2021). Despite the increasing number of reports with BIN2 acting as an essential regulator in growth/stress balance, no multi-omics studies on this kinase have been reported so far.

In Arabidopsis thaliana, the TARGET OF RAPAMYCIN complex (TORC) is an important regulator that integrates nutrient and energy sensing into cell proliferation and growth (Xiong & Sheen, 2014; Fu et al., 2020). Activation of TORC signaling induces the expression of ribosomal proteins, increases protein translation, photosynthesis, and upregulates (transcriptionally and translationally) plant growthpromoting genes (Ren et al., 2012; Xiong et al., 2013; Dong et al., 2015; Van Leene et al., 2019; Scarpin et al., 2020). Conversely, TORC actively represses autophagy, a central recycling system of cytoplasmic components that is essential for rerouting nutrients and other raw materials when needed for plant growth, development, or stress responses (Noda & Ohsumi, 1998; Pu et al., 2017; Marshall & Vierstra, 2018). TORC is comprised of TOR kinase, LETHAL WITH SEC THIRTEEN PROTEIN 8 (LST8), and REGULATORY ASSOCIATED PROTEIN OF TOR (RAPTOR). TOR is the catalytic component of TORC, LST8 provides stability, and RAPTOR interacts with and recruits substrates to the complex (Hara et al., 2002; Mahfouz et al., 2006; Yang et al., 2013). In Arabidopsis, null mutants in *TOR* are embryo lethal (Menand et al., 2002). Arabidopsis has two RAPTOR homologs, RAPTOR1A and RAPTOR1B, with RAPTOR1B being the predominantly expressed paralog (Deprost et al., 2005; Anderson et al., 2005). Loss of RAPTOR1A has no impact on plant growth and development while raptor1b plants have reduced TORC activity, impaired morphogenesis, and increased basal autophagy (Anderson et al., 2005; Pu et al., 2017; Wang et al., 2018; Salem et al., 2018). The combined loss of raptor1a raptor1b double mutant embryos are viable and plants maintain embryonic development, unlike tor mutants, but lack post-embryonic growth (Anderson et al., 2005).

When plants encounter stress, autophagy is often triggered, and growth-promoting pathways such as BR or TORC signaling need to be dampened (Nolan *et al.*, 2017b; Liao & Bassham, 2020). To enable this balanced regulation of plant growth and stress

responses, hormonal pathways such as auxin (Li et al., 2017; Schepetilnikov et al., 2017) and BRs (Zhang et al., 2016; Vleesschauwer et al., 2018) can influence or be affected by TORC activity. Increasing evidence points towards TORC-regulated autophagy as a crucial interaction point between BRs and TORC signaling when controlling this balance. For example, activation of TORC signaling promotes BR response by stabilizing BZR1, likely preventing its autophagy-driven degradation (Zhang et al., 2016). Additionally, BIN2 knock-down lines exhibit reduced sensitivity to TOR inhibitors AZD8055 (AZD) and KU63794 (Xiong et al., 2017). Furthermore, RIBOSOMAL PROTEIN S6 KINASE 2 (S6K2) can phosphorylate BIN2 in a TOR-dependent manner. However, the mechanism and biological implications of this interaction are not clear (Xiong et al., 2017). Under stress conditions such as drought or sucrose starvation, BES1 is ubiquitinated by SINAT2 and/or BAF1 ubiquitin ligases and targeted to selective autophagy through ubiquitin receptor DSK2 to slow down plant growth (Nolan et al., 2017a; Yang et al., 2017; Wang et al., 2021). Moreover, BIN2 has been shown to phosphorylate ubiquitin receptor DSK2 to facilitate its interaction with ATG8 and promote BES1 degradation via selective autophagy (Nolan et al., 2017a).

BIN2 and TORC regulate plant responses to environmental changes via phosphorylation, exerting molecular changes at many different levels (i.e., changes in gene transcription or protein activity) (Guo et al., 2013; Youn & Kim, 2015; Bozhkov, 2018; Van Leene et al., 2019; Nolan et al., 2020; Liao & Bassham, 2020). Therefore, understanding the molecular connection between BR and TORC signaling across different levels of gene expression is necessary to unravel the interplay between these pathways. Furthermore, despite BIN2 being intensively studied, proteome-wide identification of BIN2 substrates is lacking. Here, we present a comprehensive multi-omic profiling detailing transcriptome, proteome, and phosphoproteome changes that occur in mutants with altered levels of BIN2 or the TORC subunit RAPTOR1B. We complement these global *in vivo* profiles with proteome-wide identification of direct BIN2 substrates using a Multiplexed Assay for Kinase Specificity (MAKS). Substantial overlap was found in the transcripts, proteins, and phosphosites whose accumulation is dependent on BIN2 and RAPTOR1B. Using this wealth of information, we reconstructed an integrated kinase-signaling network and gene regulatory network (GRN). We used this integrated network to identify novel genes whose

mutant lines showed either altered growth in response to BR and/or levels of autophagy. Together, these studies further our understanding of the dynamic interplay between BR and TORC signaling.

Materials and Methods

Plant material

Arabidopsis thaliana (L.) Heynh. mutant lines bin2-1 (Li & Nam, 2002), bin2-3 bil1 bil2 (Yan et al., 2009), and raptor1-1 (Deprost et al., 2005; Anderson et al., 2005) were used in this research as bin2D, bin2T, and raptor1b, respectively. The full list of seed stocks used in this work are summarized in Supporting Information Dataset S1. All plants were grown in LC1 soil mix (Sungro) under long day conditions (16 h : 8 h, light : dark, 22°C) unless stated otherwise. Columbia-0 ecotype was used as wild-type control for all assays.

QuantSeq library preparation and sequencing

Four biological replicates of 20-day-old rosette leaves were collected from WT and each mutant (*bin2T*, *bin2D*, and *raptor1b*) and immediately frozen in liquid N₂. Tissue was ground for at least 15 minutes under liquid N₂ using mortar and pestle. Total RNA was extracted using RNAeasy Plant Mini Kit with DNasel treatment (Qiagen). Five-hundred ng of total RNA was used for QuantSeq 3' mRNA-seq library Prep kit FWD for Illumina (Lexogen) (Moll *et al.*, 2014). Library sequencing was performed on an Illumina HiSeq3000 at the ISU DNA facility.

Transcriptomic data analysis

QuantSeq 3' mRNA-seq Integrated Data Analysis Pipeline on Bluebee® Genomic Platform User Guide (Lexogen Cat. 090-094) was followed. Reads were adapter- and quality-trimmed using BBDuk v37.36. Trimmed reads were mapped to the Arabidopsis reference transcriptome (TAIR10 annotation) using Star Aligner v2.5.3a (Dobin *et al.*, 2013). Finally, transcript counts were extracted using HTSeq-count v0.11.2 (Anders *et al.*, 2015).

Differential expression was assessed using the PoissonSeq R package (Li *et al.*, 2012). A q-value < 0.05 and fold change > 1.3 (Log₂FC > 0.4) was used as cutoff for designating

differentially expressed transcripts. All data processing scripts were deposited in a github repository (see Data Availability section).

Protein extraction for global proteome and phosphoproteome profiling

Three biological replicates from the same tissue collected for transcriptome analysis were processed for (phospho)proteomic profiling based on established methods (Song *et al.*, 2018b,a, 2020). Protein was extracted using the urea-FASP method from 250 mg of finely ground tissue. Tandem Mass Tag (TMT lot #TC264166, Thermo Scientific) labeling was performed on 330 µg of purified peptides from each sample in a 1:1.7 (peptide:label) ratio as previously reported (Song *et al.*, 2020). TMT labeling reaction efficiency was assessed to be at least of 98% by liquid chromatography-tandem mass spectrometry (LC-MS/MS). Labelling reaction was quenched using 5% hydroxylamine and the samples were then pooled. One hundred µg of labeled peptide was used for global proteome profiling and the remaining labeled sample was subjected to a second round of C18 desalting before phosphopeptide enrichment via Serial Metal Oxide Affinity Chromatography (SMOAC) using High-Select TiO₂ and Fe-NTA enrichment (Thermo Scientific). Full protein extraction methods are detailed in Supporting Information Methods S1.

BIN2 Multiplexed Assay for Kinase Specificity (MAKS)

MAKS was performed based on the protocol described by (Jayaraman *et al.*, 2017) using protein extracted from 1 g of 20-day-old leaf Col-0 tissue using the phenol-FASP protocol (Song *et al.*, 2018b, 2020). Three mg of total purified protein was resuspended in urea resuspension buffer (8 M urea in 50 mM TRIS-HCl, pH = 7.0; 5 mM TCEP), re-precipitated in ice-cold 100 mM NH₄CH₃CO₂ in 100% methanol. Following precipitation, the solvent was removed and the protein pellet was resuspended in kinase buffer (50 mM TRIS-HCl, pH = 7.7; 5 mM MgCl₂; 5mM ATP; 1x phosphatase inhibitor cocktail). Resuspended protein was divided into 600 μg aliquots and incubated with either recombinant GST or GST-BIN2 at a 1:75 (enzyme:protein) ratio at 37°C with gentle shaking for 1 hour. After incubation, protein solution was subjected to FASP, reduced with 2mM TCEP, alkylated in 50mM IAM, and digested using trypsin as described by (Song *et al.*, 2020). Three replicates were analyzed for each treatment (i.e., GST and GST-BIN2). Two hundred μg of peptides from each replicate were used for TMT labeling. Phosphopeptide enrichment

was performed on labeled peptides using SMOAC. GST-BIN2 was previously cloned (Yin et al., 2002) and purified using glutathione agarose beads as described in (Jiang et al., 2019).

LC-MS/MS

Two-dimensional liquid chromatography-tandem mass spectrometry (2D-LC-MS/MS) was performed on an Agilent 1260 quaternary HPLC coupled to a Thermo Scientific Q-Exactive Plus high-resolution quadrupole Orbitrap mass spectrometer (Song *et al.*, 2018a; Zhang *et al.*, 2019; Clark *et al.*, 2021). Full LC-MS/MS methods are detailed in Supporting Information Methods S2.

Proteomics data analysis

Spectra for global protein abundance runs were searched using the Andromeda Search Engine (Cox et al., 2011) against the TAIR10 Arabidopsis proteome using MaxQuant software v1.6.1.0 (Tyanova et al., 2016). Carbamidomethyl cysteine was set as a fixed modification while methionine oxidation and protein N-terminal acetylation were set as variable modifications. Digestion parameters were set to 'specific' and 'Trypsin/P;LysC'. Up to two missed cleavages were allowed. A false discovery rate less than 0.01 at both the peptide spectral match and protein identification level was required. Sample loading (SL) and internal reference scaling (IRS) normalization methods were used to account for differences within and between 2D-LC-MS/MS runs, respectively (Plubell et al., 2017).

Differential expression was assessed using the PoissonSeq R package (Li *et al.*, 2012). A q-value < 0.1 was used as cutoff for designating differentially expressed proteins. Scripts for data analysis were deposited in a github repository (see Data Availability section)

Phosphoproteomics data analysis

Spectra for both *bin2/raptor1b* mutant profiling and MAKS were searched together using the same approach as for global protein abundance with exceptions. Briefly, MaxQuant software v1.6.10.43 was used instead and 'Phospho (STY)' search for variable

modifications was included. SL and IRS normalization methods were used to account for differences within and between 2D-LC-MS/MS runs, respectively (Plubell *et al.*, 2017).

Differential expression was assessed using the edgeR R package (Robinson *et al.*, 2010). A q-value < 0.1 was used as cutoff for designating differential phosphorylation. See Data Availability section for the full analysis script.

Motif enrichment analysis

Motif enrichment was performed using the motifeR R package (Wang *et al.*, 2019) with default settings: serine or threonine as the central residues, a p-value threshold of 0.001, a search window of 15 amino acids (AAs) upstream and downstream of selected phosphosite for a final 31 AAs sequence window, and TAIR10 protein annotation as background reference. Enrichment p-value was calculated by hypergeometric testing using *phyper* function in R.

Analysis of overlap between BIN2 MAKS and bin2 mutant datasets.

To find overlapping phosphosites, we defined any two distinct phosphosites as identical if they originated from the same phosphoprotein and were less than 10 amino acid residues apart. This approach was used to account for cases where phosphosites were not localized to a specific amino acid on a given peptide in the two different datasets. Overlap statistical significance was assessed by hypergeometric test.

Kinase activation loop prediction

Protein kinases were identified using a modified version of the pipeline described by (Walley *et al.*, 2013). Briefly, all 35,386 protein sequences available in the TAIR10 annotation were searched for kinase domain using The National Center for Biotechnology Information batch conserved domain search tool (Lu *et al.*, 2020). From this list of 1,522 proteins with identified kinase domain, 878 were also annotated with activation loop (A-loop) coordinates by the search tool. The kinase domains of proteins lacking the A-loop coordinates were aligned using MAFFT (Katoh & Standley, 2013) and the well conserved A-loop beginning (DFG) and end (APE) motifs were manually searched. An extra 482 A-

loop coordinates were obtained, for a total of 1,360 protein kinases with A-loop coordinates.

Kinase-signaling network

Kinases with differential phosphorylation inside the A-loop (activated kinases) were used as regulators to build the kinase-substrate network. For this, the Spearman and Pearson correlation between a regulator and the rest of differentially phosphorylated peptides was calculated as described previously (Supporting Information Fig. S2b, see later) (Walley et al., 2013; Clark et al., 2021).

Gene Regulatory Network reconstruction

A curated list of transcriptional regulators was used to identify quantified TFs in our datasets (Supporting Information Dataset S2) For the abundance GRN, TF protein abundance (when quantified) or TF transcript abundance (when cognate protein was not quantified) was used as the 'regulator' value to infer their 'target' transcript abundance. The phosphosite GRN, uses the TF phosphorylation intensity value as 'regulator' to predict 'target' transcript abundance. In order to mix different data sources (i.e., proteomics, phosphoproteomics, and transcriptomics) into consolidated tables, expression values for each 'omics' were rank-normalized using the *norm.rrank* function from the r package 'demi' (Ilmjärv *et al.*, 2014). In both networks, transcript abundance was used to build the target tables.

Network inference was achieved using a modified version of the GENIE3 random forest algorithm (Huynh-Thu *et al.*, 2010) in the SC-ION pipeline V2.1 (https://doi.org/10.5281/zenodo.5237310) with no clustering, as described before (Clark *et al.*, 2021). Results were visualized in Cytoscape v3.9.0 (Shannon *et al.*, 2003)

IVI score was calculated using the 'influential' and 'igraph' r packages following developer instructions (Csardi & Nepusz, 2006; Salavaty *et al.*, 2020). A table with all the network interactions, where the first column had the regulator's gene ID and the second column had the corresponding target's gene ID, was parsed using an in-house script (See Data Availability section for the full analysis script).

BL response assays

Seeds were vapor-phase sterilized in chlorine gas, stratified at 4°C for 1 week, and germinated in on petri plates containing half-strength Linsmaier and Skoog media (1/2 LS, Caisson Labs, catalog number LSP03) in 0.7% Phytoblend (Caisson Labs, catalog number PTP01), supplemented with 1% sucrose and either DMSO or 100 nM brassinolide (BL). Seedlings were grown for 7 days at 22 °C : 18 °C, day : night, and 16 h : 8h, light : dark, 40% relative humidity, and light intensity of 120 µmol m⁻² s⁻¹. Seedlings were imaged and hypocotyl length was measured using Fiji software (Schindelin *et al.*, 2012). Twenty-four seedlings per mutant were used on each treatment and this experiment was repeated at least two times for those genotypes showing significant response. A generalized linear model with treatment and genotype as factors and controlling for random effects of replicate and plate was applied using the *glmmPQL* function from the MASS R package (Venables & Ripley, 2002), and a threshold of 'genotype by treatment interaction'. A p-value < 0.1 in each of two independent experiments was set as the significance cutoff.

GFP-ATG8e protoplast assay

Protoplasts were isolated from 20-day-old leaves and transformed as described previously (Wu *et al.*, 2009). Protoplasts were observed by epifluorescence microscopy (Carl Zeiss Axio Imager.A2, Germany) using a FITC filter, and protoplasts with more than three visible autophagosomes were counted as active for autophagy as previously described (Yang *et al.*, 2016; Pu *et al.*, 2017). One hundred protoplasts were analyzed per treatment per genotype and the experiment was repeated three times. For sucrose starvation, transformed protoplasts were incubated in W5 solution without sucrose or with 0.5% (w/v) sucrose as control at room temperature for 36 hours in dark before assessing autophagy.

Significance of basal autophagy levels was assessed by two-sample t-test whereas a generalized linear model with treatment and genotype as factors and controlling for random effects of replicates was used for autophagy levels under sucrose starvation. A p-value < 0.05 was used as a cutoff on both cases.

Western Blotting

For BES1 western blot, 10-day-old seedlings were grown on ½ LS plates under constant light and then transferred to either liquid ½ LS or ½ LS with 100 nM BL for 2 hours. Seedlings were collected, dabbed dry, and flash frozen in liquid nitrogen. Samples were ground in 2x SDS buffer (100 mM Tris–HCl pH 6.8, 4% (w/v) SDS, 20% (v/v) glycerol, 0.2% (w/v) bromophenol blue, 0.2 M β -mercaptoethanol) and resolved on 8% SDS-PAGE followed by western blotting with anti-BES1 antibody.

S6K western blot was done similar to BES1, with the exception that 7-day-old seedlings were grown on $\frac{1}{2}$ LS plates under constant light and then transferred to either liquid $\frac{1}{2}$ LS or $\frac{1}{2}$ LS with $\frac{1}{4}$ M AZD8055 for 2 hours. And blotted using anti-S6K1/2 antibody (Agrisera, AS12 1855).

Results

Multi-omics profiling of *bin2* and *raptor1b* mutants provides insights into known and new regulatory roles.

To discover novel molecular components linked to BR and/or TORC signaling we performed quantitative multi-omics. We performed transcriptome, proteome, and phosphoproteome profiling on rosette leaves of 20-day-old wild-type (WT), bin2D (gainof-function), bin2T (bin2 bil1 bil2 triple loss of function), and raptor1b loss of function plants. We quantified transcript levels using 3' QuantSeq (Moll et al., 2014) and measured abundance phosphorylation using two-dimensional protein and state chromatography-tandem mass spectrometry (2D-LC-MS/MS) on Tandem Mass Tag (TMT) labeled peptides (McAlister et al., 2012; Song et al., 2018a; Hogrebe et al., 2018) (Fig. 1a). From these samples, we detected 23,975 transcripts, 11,183 proteins, and up to 27,887 phosphosites from 5,675 phosphoproteins (Fig. 1b and Supporting Information Dataset S3). We found 5,653 transcripts and 4,001 protein groups (hereafter referred to as proteins) that were differentially expressed (DE) in at least one mutant when compared to WT (Fig. 1c and Supporting Information Fig. S1a,b). Gene ontology (GO) analysis of DE transcripts and proteins in bin2D, bin2T, and raptor1b mutants showed enrichment of many terms from similar processes including growth, hormones, stimuli sensing, and stress (Fig. 2a,b; Supporting Information Datasets S4 and S5), which is consistent with the known roles of BIN2 and RAPTOR in growth/stress balance and hormonal crosstalk.

Our phosphoproteomics analysis identified 4,153 differentially phosphorylated sites in at least one mutant (Fig. 1c, Supporting Information Dataset S3c, and Supporting Information Fig. S1c). GO analysis for potential BIN2 target proteins (i.e., those with increased phosphorylation in *bin2D* or decreased phosphorylation in *bin2T*) revealed enrichment of terms related to plant growth and development, as well as response to stress and defense, processes in accordance with known functions of BIN2 and its homologs. In addition, response to BR, abscisic acid, and auxin terms were also significant, highlighting once more the close relationship between BIN2 activity and these hormones. Transcriptional regulation-related terms were significantly enriched in the *bin2D* dataset, consistent with known impacts of BIN2 on transcription factors (TFs) (Fig.

2c and Supporting Information Dataset S6). Finally, we assessed GO enrichment for proteins with decreased phosphorylation in *raptor1b*. We found that most of the enriched terms were related to growth, autophagy, starvation, auxin, and BR response. This is consistent with the known biological role of RAPTOR and suggests a cross-regulation between BR and TORC pathways via phospho-signaling (Fig. 2c and Supporting Information Dataset S6).

Phosphoproteomic analysis of *bin2* mutants shows enrichment of BIN2 direct targets.

Because BIN2 is a kinase, we hypothesized that phosphosites increased in the bin2D gain-of-function mutant or decreased in bin2T may be direct BIN2 substrates. To test this hypothesis, we generated a proteome-wide dataset of BIN2 direct targets using the multiplexed assay for kinase specificity (MAKS) (Brumbaugh et al., 2014; Jayaraman et al., 2017) (See Methods for details). We quantified a total of 10,375 phosphosites accounting for 3,628 phosphoproteins from this assay (Supporting Information Dataset S3c). As expected, the obtained phosphoproteome was heavily skewed toward increased phosphosites, with 1,343 phosphosites increasing following incubation with GST-BIN2 (Fig. 3a and Supporting Information Dataset S3c). Among proteins with increased phosphorylation we observed YDA and BSK1, two known BIN2 targets (Kim et al., 2012; Sreeramulu et al., 2013). To evaluate this set of phosphorylation sites as BIN2 kinasesubstrates, we performed motif enrichment analysis and found a significant enrichment of the well-known GSK3 motif 'S/T-X-X-S/T' (Fiol et al., 1987; Youn & Kim, 2015) among the increased phosphosites (P < 0.01, Fig. 3b and Supporting Information Dataset S7a). Additionally, another highly enriched motif found in the analysis was 'S/T-P', which is reported as a motif for GSK3, CDK, and MAPK families (Amanchy et al., 2007; Lin et al., 2015) (Supporting Information Dataset S7a). Some previously unreported length variations of the GSK3 motif were also significantly enriched (i.e., S/T-X-X-S/T, S/T-X-S/T, and S/T-S/T, Supporting Information Dataset S7a). These results support the robustness of our BIN2 kinase dataset and suggest a more flexible substrate recognition motif for BIN2 as a GSK3-like kinase.

We next assessed the prevalence of BIN2 direct targets present in our *in vivo* profiling of bin2D and bin2T mutants. For this, we first performed motif enrichment analysis on phosphosites perturbed in the expected direction for BIN2 targets (i.e., either upregulated in bin2D or downregulated in bin2T). A significant enrichment for the GSK3 motif was found in both bin2D up (P < 0.01) and bin2T down (P < 0.01) phosphosites (Fig. 3b and Supporting Information Dataset S7b,c). Next, we looked at the overlap with BIN2 direct targets identified in the MAKS experiment. For bin2D, 17.0% (41/241; P < 0.01) of the total differentially upregulated phosphosites and 23.6% (38/161; P < 0.01) of the upregulated phosphoproteins were also BIN2 direct targets. For bin2T, 13.8% (77/558; P < 0.05) of the downregulated phosphosites and 23.3% (117/503; P < 0.01) of the downregulated phosphoproteins were also part of our BIN2 direct substrate list (Fig. 3c and Supporting Information Dataset S8). These results indicate that a subset of the BIN2-dependent phosphosites identified by in vivo mutant profiling may be direct BIN2 substrates.

Kinase-signaling network inference on bin2 and raptor1b mutants.

Since both BIN2 and RAPTOR1B (TORC) participate in phosphorylation-based signaling, we reconstructed the molecular relationships of these signaling networks. To do so, we used our data to infer a kinase-signaling network for each mutant (i.e., bin2D, bin2T, and raptor1b). To build these networks, we inferred the activation state of kinases in our dataset. The activation loop (A-loop) is a well-conserved region inside the kinase domain whose phosphorylation is necessary for kinase activation (Adams, 2003; Ahiri, 2019). Thus, phosphosite intensity level of the A-loop can be used as a proxy for kinase activity quantification (Walley et al., 2013; Beekhof et al., 2019; Schmidlin et al., 2019; Clark et al., 2021). First, we performed a whole-proteome Arabidopsis in-silico A-loop prediction and were able to identify this region on 1,360 proteins (Supporting Information Dataset S9a). Subsequently, we identified kinases whose A-loop phosphosite intensity was differentially regulated in at least one of the profiled mutants (Supporting Information Fig. S2a and Supporting Information Dataset S9b).

We found 27, 21, and 24 kinases exhibiting an altered activation state in the *bin2D*, *bin2T*, and *raptor1b* mutants, respectively (Supporting Information Dataset S9b). Using this

information, we inferred a kinase-signaling network by correlating phosphosite level with kinase activation state (Supporting Information Fig. S2b). A network containing 4,138 nodes, representing 33 activated kinases and 2,284 target sites arising from 1,853 possible substrate proteins was obtained (Fig. 4a and Supporting Information Dataset S10). To evaluate this kinase-signaling network, predicted BIN2 targets were obtained (i.e., nodes connected by edges directed outward of BIN2), and motif enrichment analysis was performed. As expected, the GSK3 motif was enriched among BIN2 targets (P = 1.96e-06). Additionally, the MAPK consensus motif P-X-[pS/pT]-P was overrepresented among MPK6 targets (P < 0.01). Several variants of the proline-directed phosphorylation motif [pS/pT]-P were significantly enriched among targets of MPK4 (P < 0.001), MPK10 (P < 0.001), and BIN2 (P < 0.001) (Amanchy et al., 2007; Lin et al., 2015; Rayapuram et al., 2021) (Fig. 4b and Supporting Information Dataset S11). Finally, 70% (7/10) of known BIN2 targets reported in the literature and present in our network were correctly predicted as BIN2 targets (either as direct targets or direct downstream second neighbor, Supporting Information Dataset S10b). These results support the target prediction value of our inferred kinase signaling network.

Integrative multi-dimensional signaling network reconstruction reveals proteins required for normal BR response and autophagy.

We have previously shown that using multiple omics datasets can increase the predictive power of Gene Regulatory Network (GRN) inference (Walley *et al.*, 2016). We inferred two separate transcription factor (TF)-centered GRNs using the SC-ION pipeline (Fig. 5) (Clark *et al.*, 2021). In the 'abundance GRN', TF protein abundance (when quantified) or TF transcript abundance (when cognate protein was not quantified) was used as the 'regulator' value to infer their 'target' transcript abundance. (Fig. 5, blue line). In the 'phosphosite GRN', the quantified TF phosphorylation intensity value was used as a 'regulator' to predict 'target' transcript abundance (Fig. 5, green line). These two GRNs were integrated with the kinase-signaling network to provide a multi-layered portrait of signaling cascades dependent on BR and TOR (Fig. 5; Supporting Information Dataset S12). In this network, there are 2,272 BIN2-responsive nodes (kinases, regulatory TFs, or targets) that are present based on regulatory inference being made using information

from mutants with altered BIN2 levels (Fig. 5, left side) and 2,370 RAPTOR1B/TORC-dependent nodes (Fig. 5, right side). Additionally, 1,044 nodes are linked to both BIN2 and RAPTOR1B, elucidating novel molecular connections between both pathways (Fig. 5, center). To identify important network regulators, we calculated the Integrated Value of Influence (IVI) score for each node, which integrates network centrality measurements into one normalized value to account for each node's ranked importance in the analyzed network (Salavaty et al., 2020) (Table 1, Supporting Information Dataset S12b). Among the top 10% most influential nodes, we observed well-known BR signaling regulators such as BAK1, BEH1, BES1, BIM1, BIN2, and BSK1, as well as previously reported TOR targets such as VIP1, RBR1, and HAG1 (Van Leene et al., 2019).

Next, we examined the integrative signaling network to determine whether these predictions identified proteins involved in BR response and/or TORC-response. To assess this question, we enlisted those proteins being differentially phosphorylated simultaneously in either of the BIN2 mutants (i.e., bin2D or bin2T) and in raptor1b (Fig. 6). When selecting candidates, we focused our attention on the 1,044 'co-regulated' genes present in the integrative network (Fig. 5, center). We next filtered to keep those proteins up-phosphorylated in bin2D and those down-phosphorylated in bin2T since this phosphorylation 'directionality' could pinpoint those proteins direct or indirectly affected by BIN2 activity. Finally, we fine-tuned this selection to identify possible BIN2/RAPTOR1B co-regulated genes by keeping only those proteins exhibiting differential phosphorylation in raptor1b (Fig. 6). This selection criteria gave us a total of 48 candidate genes. We were able to obtain viable mutants for 41 of these genes to perform a reverse genetic screen for altered BR responses and autophagy phenotypes (Supporting Information Dataset S13). In BR induced hypocotyl elongation assays mutants in 31.7% (13/41) of the genes showed a significantly altered BL response (Fig. 7, and Supporting Information Dataset S13a). To place the 13 genes with altered hypocotyl growth as upstream or downstream of BES1 we measured BES1 phosphorylation state in these mutants by western blotting. BES1 accumulation in the unphosphorylated form in response to BL still happens in most tested mutants and no obvious relationship between BL effect on hypocotyl growth and BES1 phosphorylation changes upon BL treatment were noticed, suggesting that perturbations on these mutants happen downstream of or in parallel with BES1. The

mechanisms by which these genes affect BR responses remain to be determined in future studies (Supporting Information Fig. S3). We next measured autophagy levels as a readout of TORC activity, a total of 29 candidate genes that showed significantly altered hypocotyl elongation in response to BL and/or exhibited decreased phosphorylation in raptor1b mutant were examined for autophagy activity by transient expression of a GFP-ATG8e marker, which labels autophagosomal membranes, in protoplasts obtained from mutant lines (Contento *et al.*, 2005). Twenty genes (71.4% of assayed candidate genes) showed significantly altered basal autophagy levels when mutated, with 15 of them being higher than WT and five lower than WT (Fig. 8 and Supporting Information Dataset S13b). GFP-ATG8e was also assessed under sucrose starvation for the same genotypes. Nineteen genes (67.9% of assayed genes) showed significant changes in autophagosome number under sucrose starvation conditions. Interestingly, there was little to no increase in autophagy upon sucrose starvation in the five genotypes with low basal autophagy (Fig. 8 and Supporting Information Dataset S13b). We further examined the mutants showing altered autophagy by assessing phosphorylation of S6K, a known TORC substrate, by western blot (Supporting Information Fig. S4). Most of the mutants showed no clear difference in S6K phosphorylation when compared to WT. However, 3 out of the 20 assayed genotypes (ref6-1, at3g01160-1, and pin4-3) showed a noticeable reduction in phospho-S6K which was consistent with their corresponding GFP-ATG8e autophagy levels. This suggests that most of these genes act downstream of TORC. Nevertheless, three of our mutants seem to work upstream of TORC to negatively regulate autophagy.

In summary, we found a total of 26 genes out of the 41 selected candidates (63.4%) showing an altered response to BR and/or level of autophagy with 11 of them presenting both BR and autophagy phenotypes. We, moreover, found three genes whose mutation can affect TORC activity. These results confirm the robustness of our integrative multi-omics approach as a way of selecting candidate proteins related to the brassinosteroid and/or autophagy pathways.

Discussion

Brassinosteroid and TORC have emerged as two key signaling pathways coordinating growth and stress responses. An outstanding question in the field is the interplay between these two pathways across levels of gene expression. By quantifying multi-omics data across key genotypes, we generated a kinase-signaling network and two TF-centric GRNs. These networks were then merged into one integrative multi-dimensional network, which predicted novel genes that function in both shared and unique BR-TORC pathways. These data were validated with several reverse genetic screens to uncover novel players of BR, TOR and BR-TORC responses *in vivo*.

Our work supports previous transcriptome profiling studies of BR (Wang et al., 2014; Kim et al., 2019; Liu et al., 2020) and TOR signaling (Ren et al., 2012; Xiong et al., 2013; Dong et al., 2015). In addition, this study provides comprehensive phosphoproteomic data underpinning BR signaling via BIN2. Furthermore, a global catalogue of potential direct BIN2 substrates was generated using MAKS. In terms of TORC signaling, we substantially expand on the work of Salem et al., which provided an initial description of proteins that are mis-expressed in *raptor1b* (Salem et al., 2018) as well as the proteins and phosphorylation sites that respond to TOR inhibition via treatment with Torin 2, AZD8055, or rapamycin (Van Leene et al., 2019; Scarpin et al., 2020). Most importantly, through the generation and analysis of these multi-omics data we found a large overlap of gene-products (i.e., transcript, protein, or phosphosites) whose level is altered in response to the misexpression of both BIN2 and RAPTOR1B. Additionally, 22 of the potential BIN2 substrates identified in the MAKS experiment were previously identified by Van Leene et al. (2019) as TORC targets. Together our data suggest extensive interplay between BR- and TORC- dependent signaling pathways.

Using our multi-omics data, we reconstructed an integrated gene regulatory and kinase-signaling network. By focusing on the 1,044 regulators and targets predicted by this regulatory network to be co-regulated by BIN2 and RAPTOR1B (Fig. 5, center), and accounting for the phosphosites fold-change 'directionality' on each mutant (Fig. 6), we identified and tested a set of 41 candidate genes for their involvement in BR/TORC signaling pathways.

To summarize these phenotyping results, we divided our gene set into groups according to their different phenotypes in BR-regulated hypocotyl elongation and autophagy levels as a readout of TORC activity (Fig. 9). TOR signaling is known to be positively regulated by auxin and glucose availability (Xiong et al., 2013; Li et al., 2017; Schepetilnikov et al., 2017). Here, we found that loss of the auxin efflux carrier PIN4 (Friml et al., 2002) exhibited increased autophagy and reduced TOR activity (Fig. 9, purple). In additional, we discovered homologs of proteins involved in autophagy and mTOR signaling in human. Homo sapiens (Hsa) PTEN has been shown to negatively regulate both mTOR signaling and autophagy through independent pathways (Errafiy et al., 2013). In agreement, our results show that Arabidopsis PTEN3 mutant plants have increased autophagy (Fig. 9, purple). Conversely, HsaHMGB1 can translocate to the cytoplasm and induce autophagy upon perception of reactive oxygen species (Tang et al., 2010). Here, AtHMGB1 mutants show reduced sensitivity to BR and increased autophagy levels (Fig. 9, dark green), suggesting an opposite function in plants.

Finally, our results identified novel components of BR and autophagy pathways *in planta*. For example, loss of MPK6 leads to reduced BR sensitivity and increased autophagy levels (Fig. 9, dark green). Although no direct role as a BR-induced growth has been established, MPK6 kinase is involved in a myriad of processes and has been shown to directly phosphorylate and activate BES1 to increase immune response (Kang *et al.*, 2015). Furthermore, BIN2 can phosphorylate and inhibit MKK4, a direct MPK6 activator (Khan *et al.*, 2013). Moreover, our signaling network prediction situates MPK6 as potentially being upstream of RAPTOR1B.

In summary, this study builds upon previous findings that connect BR and TORC in the regulation of plant growth and stress responses (Zhang *et al.*, 2016; Xiong *et al.*, 2017; Nolan *et al.*, 2017a, 2020; Vleesschauwer *et al.*, 2018; Liao & Bassham, 2020). Our multiomics studies provide genome-wide evidence for extensive interactions between BR and TORC signaling pathways across different gene expression levels. These results establish an integrative signaling network that defines molecular interactions between BR- or TORC-regulated growth and autophagy.

Acknowledgements

This work was supported by the lowa State University Plant Science Institute (YY and JW), NIH R01GM120316 (YY, DB, JWW), NSF IOS-1818160 (YY and JW), and USDA NIFA Hatch project IOW3808 funds to JWW. NMC is supported by a USDA NIFA Postdoctoral Research Fellowship (2019-67012-29712) and TMN is supported by the National Science Foundation Postdoctoral Research Fellowships in Biology Program (Grant No. IOS-2010686). We thank Peng Liu (ISU Department of Statistics) for help in determining statical analysis for the BL and autophagy phenotype assays.

Author Contributions

CM, TMN, HG, DCB, YY, and JWW planned and designed the research. CM, PW, C-YL, TMN, GS, NMC, and JME performed experiments and analyzed data CM, TMN, DCB, YY, and JWW wrote the manuscript.

Data Availability

The RNA-seq data generated by this work has been deposited at the National Center for Biotechnology Information (NCBI) Short Read Archive (SRA) as BioProject accession number PRJNA678744.

The original MS proteomics raw data, as well as the MaxQuant output files, can be downloaded from MassIVE (http://massive.ucsd.edu) using the identifier MSV000086460 for *bin2D*, *bin2T*, and *raptor1b* mutants profiling and MSV000086462 for the BIN2 MAKS. All the scripts used for this work are available on the following github repository: https://github.com/chrisfmontes/BIN2 RAPTOR1B MULTIOMICS.

References

Adams JA. 2003. Activation loop phosphorylation and catalysis in protein kinases: Is there functional evidence for the autoinhibitor model? *Biochemistry* **42**: 601–607.

Ahiri A 2019. Insights into evolutionary interaction patterns of the 'Phosphorylation Activation Segment' in kinase. *Bioinformation* **15**: 666–677.

Amanchy R, Periaswamy B, Mathivanan S, Reddy R, Tattikota SG, Pandey A. 2007. A curated compendium of phosphorylation motifs. *Nature Biotechnology* **25**: 285–286.

Anders S, Pyl PT, Huber W. **2015**. HTSeq--a Python framework to work with high-throughput sequencing data. *Bioinformatics* **31**: 166–169.

Anderson GH, Veit B, Hanson MR. 2005. The Arabidopsis AtRaptor genes are essential for post-embryonic plant growth. *BMC Biology* **3**: 12.

Beekhof R, van Alphen C, Henneman AA, Knol JC, Pham TV, Rolfs F, Labots M, Henneberry E, Le Large TY, de Haas RR, et al. 2019. INKA, an integrative data analysis pipeline for phosphoproteomic inference of active kinases. *Molecular Systems Biology* 15: e8250.

Bozhkov PV. 2018. Plant autophagy: mechanisms and functions. *Journal of Experimental Botany* **69**: 1281–1285.

Brumbaugh J, Russell JD, Yu P, Westphall MS, Coon JJ, Thomson JA 2014. NANOG Is Multiply Phosphorylated and Directly Modified by ERK2 and CDK1 In Vitro. *Stem Cell Reports* **2**: 18–25.

Bürger M, Chory J. 2019. Stressed Out About Hormones: How Plants Orchestrate Immunity. *Cell Host & Microbe* **26**: 163–172.

Cai Z, Liu J, Wang H, Yang C, Chen Y, Li Y, Pan S, Dong R, Tang G, Barajas-Lopez J de D, et al. 2014. GSK3-like kinases positively modulate abscisic acid signaling through phosphorylating subgroup III SnRK2s in Arabidopsis. *Proceedings of the National Academy of Sciences of the United States of America* 111: 9651–9656.

Che P, Bussell JD, Zhou W, Estavillo GM, Pogson BJ, Smith SM. 2010. Signaling from the Endoplasmic Reticulum Activates Brassinosteroid Signaling and Promotes Acclimation to Stress in Arabidopsis. *Science Signaling* 3: ra69–ra69.

Cho H, Ryu H, Rho S, Hill K, Smith S, Audenaert D, Park J, Han S, Beeckman T, Bennett MJ, et al. 2014. A secreted peptide acts on BIN2-mediated phosphorylation of ARFs to potentiate auxin response during lateral root development. *Nature Cell Biology* 16: 66–76.

Chung HY, Fujioka S, Choe S, Lee S, Lee YH, Baek NI, Chung IS. 2010. Simultaneous suppression of three genes related to brassinosteroid (BR) biosynthesis altered campesterol and BR contents, and led to a dwarf phenotype in Arabidopsis thaliana. *Plant Cell Reports* 29: 397–402.

- Clark NM, Nolan TM, Wang P, Song G, Montes C, Valentine CT, Guo H, Sozzani R, Yin Y, Walley JW. 2021. Integrated omics networks reveal the temporal signaling events of brassinosteroid response in Arabidopsis. *Nature Communications* 12: 5858.
- **Contento AL, Xiong Y, Bassham DC**. **2005**. Visualization of autophagy in Arabidopsis using the fluorescent dye monodansylcadaverine and a GFP-AtATG8e fusion protein. *The Plant Journal* **42**: 598–608.
- Cox J, Neuhauser N, Michalski A, Scheltema RA, Olsen J V., Mann M. 2011. Andromeda: A Peptide Search Engine Integrated into the MaxQuant Environment. *Journal of Proteome Research* 10: 1794–1805.
- **Csardi G, Nepusz T**. **2006**. The igraph software package for complex network research. *InterJournal* **Complex Systems**: 1695.
- **Deprost D, Truong H-N, Robaglia C, Meyer C**. **2005**. An Arabidopsis homolog of RAPTOR/KOG1 is essential for early embryo development. *Biochemical and Biophysical Research Communications* **326**: 844–850.
- Dobin A, Davis CA, Schlesinger F, Drenkow J, Zaleski C, Jha S, Batut P, Chaisson M, Gingeras TR. 2013. STAR: ultrafast universal RNA-seq aligner. *Bioinformatics* 29: 15–21.
- **Dong P, Xiong F, Que Y, Wang K, Yu L, Li Z, Ren M**. **2015**. Expression profiling and functional analysis reveals that TOR is a key player in regulating photosynthesis and phytohormone signaling pathways in Arabidopsis. *Frontiers in Plant Science* **6**: 677.
- Errafiy R, Aguado C, Ghislat G, Esteve JM, Gil A, Loutfi M, Knecht E. 2013. PTEN increases autophagy and inhibits the ubiquitin-proteasome pathway in glioma cells independently of its lipid phosphatase activity. *PloS One* 8: e83318.
- Fàbregas N, Lozano-Elena F, Blasco-Escámez D, Tohge T, Martínez-Andújar C, Albacete A, Osorio S, Bustamante M, Riechmann JL, Nomura T, et al. 2018. Overexpression of the vascular brassinosteroid receptor BRL3 confers drought resistance without penalizing plant growth. *Nature Communications* 9: 4680.
- **Fiol CJ, Mahrenholz AM, Wang Y, Roeske RW, Roach PJ. 1987.** Formation of protein kinase recognition sites by covalent modification of the substrate. Molecular mechanism for the synergistic action of casein kinase II and glycogen synthase kinase 3. *Journal of Biological Chemistry* **262**: 14042–14048.
- Friml J, Benková E, Blilou I, Wisniewska J, Hamann T, Ljung K, Woody S, Sandberg G, Scheres B, Jürgens G, et al. 2002. AtPIN4 Mediates Sink-Driven Auxin Gradients and Root Patterning in Arabidopsis. *Cell* 108: 661–673.
- **Fu L, Wang P, Xiong Y. 2020**. Target of Rapamycin Signaling in Plant Stress Responses. *Plant Physiology* **182**: 1613–1623.
- Gampala SS, Kim TW, He JX, Tang W, Deng Z, Bai MY, Guan S, Lalonde S, Sun Y, Gendron JM, et al. 2007. An Essential Role for 14-3-3 Proteins in Brassinosteroid Signal Transduction in Arabidopsis. *Developmental Cell* 13: 177–189.

- **Gruszka D**. **2018**. Crosstalk of the brassinosteroid signalosome with phytohormonal and stress signaling components maintains a balance between the processes of growth and stress tolerance. *International Journal of Molecular Sciences* **19**: 2675.
- **Guo H, Li L, Aluru M, Aluru S, Yin Y. 2013**. Mechanisms and networks for brassinosteroid regulated gene expression. *Current Opinion in Plant Biology* **16**: 545–553.
- **Gupta A, Rico-Medina A, Caño-Delgado A**. **2020**. The physiology of plant responses to drought. *Science* **368**: 266–269.
- Hara K, Maruki Y, Long X, Yoshino K ichi, Oshiro N, Hidayat S, Tokunaga C, Avruch J, Yonezawa K. 2002. Raptor, a binding partner of target of rapamycin (TOR), mediates TOR action. *Cell* 110: 177–189.
- Hogrebe A, von Stechow L, Bekker-Jensen DB, Weinert BT, Kelstrup CD, Olsen JV. 2018. Benchmarking common quantification strategies for large-scale phosphoproteomics. *Nature Communications* **9**: 1045.
- **Hu Y, Yu D**. **2014**. BRASSINOSTEROID INSENSITIVE2 interacts with ABSCISIC ACID INSENSITIVE5 to mediate the antagonism of brassinosteroids to abscisic acid during seed germination in Arabidopsis. *The Plant cell* **26**: 4394–408.
- **Huot B, Yao J, Montgomery BL, He SY. 2014**. Growth-defense tradeoffs in plants: A balancing act to optimize fitness. *Molecular Plant* **7**: 1267–1287.
- **Huynh-Thu VA, Irrthum A, Wehenkel L, Geurts P. 2010**. Inferring regulatory networks from expression data using tree-based methods. (M Isalan, Ed.). *PloS one* **5**: 10.
- Ilmjärv S, Hundahl CA, Reimets R, Niitsoo M, Kolde R, Vilo J, Vasar E, Luuk H. 2014. Estimating differential expression from multiple indicators. *Nucleic Acids Research* 42: e72.
- **Jayaraman D, Richards AL, Westphall MS, Coon JJ, Ané J-M**. **2017**. Identification of the phosphorylation targets of symbiotic receptor-like kinases using a high-throughput multiplexed assay for kinase specificity. *The Plant Journal* **90**: 1196–1207.
- **Jiang H, Tang B, Xie Z, Nolan T, Ye H, Song G, Walley J, Yin Y**. **2019**. GSK 3-like kinase BIN 2 phosphorylates RD 26 to potentiate drought signaling in Arabidopsis. *The Plant Journal* **100**: 923–937.
- Kang S, Yang F, Li L, Chen H, Chen S, Zhang J. 2015. The Arabidopsis Transcription Factor BRASSINOSTEROID INSENSITIVE1-ETHYL METHANESULFONATE-SUPPRESSOR1 is a Direct Substrate of MITOGEN-ACTIVATED PROTEIN KINASE6 and Regulates Immunity. *Plant Physiology* 167: 1076–1086.
- **Katoh K, Standley DM**. **2013**. MAFFT Multiple Sequence Alignment Software Version 7: Improvements in Performance and Usability. *Molecular Biology and Evolution* **30**: 772–780.
- Khan M, Rozhon W, Bigeard J, Pflieger D, Husar S, Pitzschke A, Teige M, Jonak C, Hirt H, Poppenberger B. 2013. Brassinosteroid-regulated GSK3/Shaggy-like Kinases Phosphorylate Mitogen-activated Protein (MAP) Kinase Kinases, Which Control Stomata Development in Arabidopsis thaliana. *The Journal of Biological Chemistry* 288: 7519–7527.

- Kim T-W, Guan S, Sun Y, Deng Z, Tang W, Shang J-X, Sun Y, Burlingame AL, Wang Z-Y. **2009**. Brassinosteroid signal transduction from cell-surface receptor kinases to nuclear transcription factors. *Nature Cell Biology* **11**: 1254–1260.
- Kim T-W, Michniewicz M, Bergmann DC, Wang Z-Y. 2012. Brassinosteroid regulates stomatal development by GSK3-mediated inhibition of a MAPK pathway. *Nature* 482: 419–422.
- Kim H, Shim D, Moon S, Lee J, Bae W, Choi H, Kim K, Ryu H. 2019. Transcriptional network regulation of the brassinosteroid signaling pathway by the BES1–TPL–HDA19 co-repressor complex. *Planta* 250: 1371–1377.
- Li X, Cai W, Liu Y, Li H, Fu L, Liu Z, Xu L, Liu H, Xu T, Xiong Y. 2017. Differential TOR activation and cell proliferation in Arabidopsis root and shoot apexes. *Proceedings of the National Academy of Sciences* 114: 2765–2770.
- **Li J, Chory J**. **1997**. A Putative Leucine-Rich Repeat Receptor Kinase Involved in Brassinosteroid Signal Transduction. *Cell* **90**: 929–938.
- **Li T, Lei W, He R, Tang X, Han J, Zou L, Yin Y, Lin H, Zhang D**. **2020a**. Brassinosteroids regulate root meristem development by mediating BIN2-UPB1 module in Arabidopsis (H Yu, Ed.). *PLOS Genetics* **16**: e1008883.
- Li J, Nagpal P, Vitart V, McMorris TC, Chory J. 1996. A role for brassinosteroids in light-dependent development of Arabidopsis. *Science (New York, N.Y.)* 272: 398–401.
- **Li J, Nam KH**. **2002**. Regulation of Brassinosteroid Signaling by a GSK3/SHAGGY-Like Kinase. *Science* **295**: 1299–1301.
- **Li J, Witten DM, Johnstone IM, Tibshirani R. 2012**. Normalization, testing, and false discovery rate estimation for RNA-sequencing data. *Biostatistics* **13**: 523–538.
- **Li J, Zhou H, Zhang Y, Li Z, Yang Y, Guo Y**. **2020b**. The GSK3-like Kinase BIN2 Is a Molecular Switch between the Salt Stress Response and Growth Recovery in Arabidopsis thaliana. *Developmental Cell* **55**: 367-380.e6.
- Liang T, Shi C, Peng Y, Tan H, Xin P, Yang Y, Wang F, Li X, Chu J, Huang J, et al. 2020. Brassinosteroid-Activated BRI1-EMS-SUPPRESSOR 1 Inhibits Flavonoid Biosynthesis and Coordinates Growth and UV-B Stress Responses in Plants. *The Plant Cell* 32: 3224–3239.
- **Liao C-Y, Bassham DC**. **2020**. Combating stress: the interplay between hormone signaling and autophagy in plants (R Mittler, Ed.). *Journal of Experimental Botany* **71**: 1723–1733.
- **Lin L-L, Hsu C-L, Hu C-W, Ko S-Y, Hsieh H-L, Huang H-C, Juan H-F. 2015**. Integrating Phosphoproteomics and Bioinformatics to Study Brassinosteroid-Regulated Phosphorylation Dynamics in Arabidopsis. *BMC genomics* **16**: 533.
- Liu X, Yang H, Wang Y, Zhu Z, Zhang W, Li J. 2020. Comparative transcriptomic analysis to identify brassinosteroid response genes. *Plant Physiology* **184**: pp.00386.2020.

- Lu S, Wang J, Chitsaz F, Derbyshire MK, Geer RC, Gonzales NR, Gwadz M, Hurwitz DI, Marchler GH, Song JS, et al. 2020. CDD/SPARCLE: the conserved domain database in 2020. *Nucleic Acids Research* 48: D265–D268.
- **Mahfouz MM, Kim S, Delauney AJ, Verma DPS**. **2006**. Arabidopsis TARGET of RAPAMYCIN interacts with RAPTOR, which regulates the activity of S6 kinase in response to osmotic stress signals. *Plant Cell* **18**: 477–490.
- **Marshall RS, Vierstra RD**. **2018**. Autophagy: The Master of Bulk and Selective Recycling. *Annual Review of Plant Biology* **69**: 173–208.
- McAlister GC, Huttlin EL, Haas W, Ting L, Jedrychowski MP, Rogers JC, Kuhn K, Pike I, Grothe RA, Blethrow JD, et al. 2012. Increasing the multiplexing capacity of TMTs using reporter ion isotopologues with isobaric masses. *Analytical Chemistry* 84: 7469–7478.
- Menand B, Desnos T, Nussaume L, Berger F, Bouchez D, Meyer C, Robaglia C. 2002. Expression and disruption of the Arabidopsis TOR (target of rapamycin) gene. *Proceedings of the National Academy of Sciences* **99**: 6422–6427.
- **Moll P, Ante M, Seitz A, Reda T**. **2014**. QuantSeq 3' mRNA sequencing for RNA quantification. *Nature Methods* **11**: i–iii.
- **Nam KH, Li J. 2002**. BRI1/BAK1, a Receptor Kinase Pair Mediating Brassinosteroid Signaling. *Cell* **110**: 203–212.
- **Noda T, Ohsumi Y. 1998**. Tor, a Phosphatidylinositol Kinase Homologue, Controls Autophagy in Yeast*. *Journal of Biological Chemistry* **273**: 3963–3966.
- Nolan TM, Brennan B, Yang M, Chen J, Zhang M, Li Z, Wang X, Bassham DC, Walley J, Yin Y. 2017a. Selective Autophagy of BES1 Mediated by DSK2 Balances Plant Growth and Survival. *Developmental Cell* 41: 33-46.e7.
- **Nolan T, Chen J, Yin Y. 2017b**. Cross-talk of Brassinosteroid signaling in controlling growth and stress responses. *The Biochemical journal* **474**: 2641–2661.
- **Nolan TM, Vukašinović N, Liu D, Russinova E, Yin Y**. **2020**. Brassinosteroids: Multidimensional Regulators of Plant Growth, Development, and Stress Responses. *The Plant Cell* **32**: 295–318.
- Planas-Riverola A, Gupta A, Betegón-Putze I, Bosch N, Ibañes M, Caño-Delgado Al. 2019. Brassinosteroid signaling in plant development and adaptation to stress. *Development (Cambridge, England)* 146: dev151894.
- Plubell DL, Wilmarth PA, Zhao Y, Fenton AM, Minnier J, Reddy AP, Klimek J, Yang X, David LL, Pamir N. 2017. Extended Multiplexing of Tandem Mass Tags (TMT) Labeling Reveals Age and High Fat Diet Specific Proteome Changes in Mouse Epididymal Adipose Tissue. *Molecular & cellular proteomics: MCP* 16: 873–890.
- **Pu Y, Luo X, Bassham DC. 2017**. TOR-Dependent and -Independent Pathways Regulate Autophagy in Arabidopsis thaliana. *Frontiers in Plant Science* **8**: 1204.

Rayapuram N, Jarad M, Alhoraibi HM, Bigeard J, Abulfaraj AA, Völz R, Mariappan KG, Almeida-Trapp M, Schlöffel M, Lastrucci E, et al. 2021. Chromatin phosphoproteomics unravels a function for AT-hook motif nuclear localized protein AHL13 in PAMP-triggered immunity. *Proceedings of the National Academy of Sciences* 118: e2004670118.

Ren M, Venglat P, Qiu S, Feng L, Cao Y, Wang E, Xiang D, Wang J, Alexander D, Chalivendra S, et al. 2012. Target of Rapamycin Signaling Regulates Metabolism, Growth, and Life Span in Arabidopsis. *The Plant Cell* 24: 4850–4874.

Robinson MD, McCarthy DJ, Smyth GK. **2010**. edgeR: a Bioconductor package for differential expression analysis of digital gene expression data. *Bioinformatics* **26**: 139–140.

Ryu H, Kim K, Cho H, Hwang I. 2010. Predominant actions of cytosolic BSU1 and nuclear BIN2 regulate subcellular localization of BES1 in brassinosteroid signaling. *Molecules and Cells* **29**: 291–296.

Ryu H, Kim K, Cho H, Park J, Choe S, Hwang I. 2007. Nucleocytoplasmic shuttling of BZR1 mediated by phosphorylation is essential in Arabidopsis brassinosteroid signaling. *Plant Cell* 19: 2749–2762.

Salavaty A, Ramialison M, Currie PD. **2020**. Integrated Value of Influence: An Integrative Method for the Identification of the Most Influential Nodes within Networks. *Patterns* **1**: 100052.

Salem MA, Li Y, Bajdzienko K, Fisahn J, Watanabe M, Hoefgen R, Schöttler MA, Giavalisco P. 2018. RAPTOR Controls Developmental Growth Transitions by Altering the Hormonal and Metabolic Balance. *Plant physiology* 177: 565–593.

Scarpin MR, Leiboff S, Brunkard JO. **2020**. Parallel global profiling of plant TOR dynamics reveals a conserved role for LARP1 in translation. *eLife* **9**: e58795.

Schepetilnikov M, Makarian J, Srour O, Geldreich A, Yang Z, Chicher J, Hammann P, Ryabova LA. 2017. GTPase ROP2 binds and promotes activation of target of rapamycin, TOR, in response to auxin. *The EMBO Journal* 36: 886–903.

Schindelin J, Arganda-Carreras I, Frise E, Kaynig V, Longair M, Pietzsch T, Preibisch S, Rueden C, Saalfeld S, Schmid B, et al. 2012. Fiji: an open-source platform for biological-image analysis. *Nature Methods* **9**: 676–682.

Schmidlin T, Debets DO, Gelder CAGH van, Stecker KE, Rontogianni S, Eshof BL van den, Kemper K, Lips EH, Biggelaar M van den, Peeper DS, et al. 2019. High-Throughput Assessment of Kinome-wide Activation States. *Cell Systems* 9: 366-374.e5.

Shannon P, Markiel A, Ozier O, Baliga NS, Wang JT, Ramage D, Amin N, Schwikowski B, Ideker T. 2003. Cytoscape: A software Environment for integrated models of biomolecular interaction networks. *Genome Research* 13: 2498–2504.

Song G, Brachova L, Nikolau BJ, Jones AM, Walley JW. **2018a**. Heterotrimeric G-Protein-Dependent Proteome and Phosphoproteome in Unstimulated Arabidopsis Roots. *PROTEOMICS* **18**: 1800323.

- **Song G, Hsu PY, Walley JW**. **2018b**. Assessment and Refinement of Sample Preparation Methods for Deep and Quantitative Plant Proteome Profiling. *PROTEOMICS* **18**: 1800220.
- **Song G, Montes C, Walley JW**. **2020**. Quantitative Profiling of Protein Abundance and Phosphorylation State in Plant Tissues Using Tandem Mass Tags. In: Jorrin-Novo JV, Valledor L, Castillejo MA, Rey M-D, eds. Methods in Molecular Biology. Plant Proteomics: Methods and Protocols. New York, NY, USA: Springer US, 147–156.
- Sreeramulu S, Mostizky Y, Sunitha S, Shani E, Nahum H, Salomon D, Hayun LB, Gruetter C, Rauh D, Ori N, et al. 2013. BSKs are partially redundant positive regulators of brassinosteroid signaling in Arabidopsis. *The Plant Journal* 74: 905–919.
- Tang D, Kang R, Livesey KM, Cheh C-W, Farkas A, Loughran P, Hoppe G, Bianchi ME, Tracey KJ, Zeh HJ, et al. 2010. Endogenous HMGB1 regulates autophagy. *Journal of Cell Biology* 190: 881–892.
- **Tyanova S, Temu T, Cox J. 2016**. The MaxQuant computational platform for mass spectrometry-based shotgun proteomics. *Nature Protocols* **11**: 2301–2319.
- Van Leene J, Han C, Gadeyne A, Eeckhout D, Matthijs C, Cannoot B, De Winne N, Persiau G, Van De Slijke E, Van de Cotte B, et al. 2019. Capturing the phosphorylation and protein interaction landscape of the plant TOR kinase. *Nature Plants* 5: 316–327.
- **Venables WN**, **Ripley BD**. **2002**. *Modern Applied Statistics with S*. New York, NY, USA: Springer.
- **Verma V, Ravindran P, Kumar PP. 2016**. Plant hormone-mediated regulation of stress responses. *BMC Plant Biology* **16**: 1–10.
- Vleesschauwer DD, Filipe O, Hoffman G, Seifi HS, Haeck A, Canlas P, Bockhaven JV, Waele ED, Demeestere K, Ronald P, et al. 2018. Target of rapamycin signaling orchestrates growth–defense trade-offs in plants. *New Phytologist* 217: 305–319.
- Walley JW, Sartor RC, Shen Z, Schmitz RJ, Wu KJ, Urich MA, Nery JR, Smith LG, Schnable JC, Ecker JosephR, et al. 2016. Integration of omic networks in a developmental atlas of maize. *Science* 353: 814–818.
- Walley JW, Shen Z, Sartor R, Wu KJ, Osborn J, Smith LG, Briggs SP. 2013. Reconstruction of protein networks from an atlas of maize seed proteotypes. *Proceedings of the National Academy of Sciences* 110: E4808–E4817.
- Wang S, Cai Y, Cheng J, Li W, Liu Y, Yang H. 2019. motifeR: An Integrated Web Software for Identification and Visualization of Protein Post-Translational Modification Motifs. *PROTEOMICS* 19: 1900245.
- Wang X, Chen J, Xie Z, Liu S, Nolan T, Ye H, Zhang M, Guo H, Schnable PS, Li Z, et al. **2014**. Histone Lysine Methyltransferase SDG8 Is Involved in Brassinosteroid-Regulated Gene Expression in Arabidopsis thaliana. *Molecular Plant* **7**: 1303–1315.
- Wang P, Nolan TM, Clark NM, Jiang H, Montes-Serey C, Guo H, Bassham DC, Walley JW, Yin Y. 2021. The F-box E3 ubiquitin ligase BAF1 mediates the degradation of the

- brassinosteroid-activated transcription factor BES1 through selective autophagy in Arabidopsis. *The Plant Cell* **33**: 3532–3554.
- **Wang Z-Y, Seto H, Fujioka S, Yoshida S, Chory J**. **2001**. BRI1 is a critical component of a plasma-membrane receptor for plant steroids. *Nature* **410**: 380–383.
- Wang P, Zhao Y, Li Z, Hsu C-C, Liu X, Fu L, Hou Y-J, Du Y, Xie S, Zhang C, et al. 2018. Reciprocal Regulation of the TOR Kinase and ABA Receptor Balances Plant Growth and Stress Response. *Molecular Cell* 69: 100-112.e6.
- Wu F-H, Shen S-C, Lee L-Y, Lee S-H, Chan M-T, Lin C-S. 2009. Tape-Arabidopsis Sandwich a simpler Arabidopsis protoplast isolation method. *Plant Methods* 5: 16.
- **Xie Z, Nolan T, Jiang H, Tang B, Zhang M, Li Z, Yin Y**. **2019**. The AP2/ERF Transcription Factor TINY Modulates Brassinosteroid-Regulated Plant Growth and Drought Responses in Arabidopsis. *The Plant Cell* **31**: 1788–1806.
- **Xiong Y, McCormack M, Li L, Hall Q, Xiang C, Sheen J. 2013**. Glucose—TOR signalling reprograms the transcriptome and activates meristems. *Nature* **496**: 181–186.
- **Xiong Y, Sheen J. 2014**. The role of target of rapamycin signaling networks in plant growth and metabolism. *Plant physiology* **164**: 499–512.
- **Xiong F, Zhang R, Meng Z, Deng K, Que Y, Zhuo F, Feng L, Guo S, Datla R, Ren M**. **2017**. Brassinosteriod Insensitive 2 (BIN2) acts as a downstream effector of the Target of Rapamycin (TOR) signaling pathway to regulate photoautotrophic growth in Arabidopsis. *New Phytologist* **213**: 233–249.
- Yan Z, Zhao J, Peng P, Chihara RK, Li J. 2009. BIN2 functions redundantly with other Arabidopsis GSK3-like kinases to regulate brassinosteroid signaling. *Plant physiology* **150**: 710–21.
- Yang M, Li C, Cai Z, Hu Y, Nolan T, Yu F, Yin Y, Xie Q, Tang G, Wang X. 2017. SINAT E3 Ligases Control the Light-Mediated Stability of the Brassinosteroid-Activated Transcription Factor BES1 in Arabidopsis. *Developmental Cell* 41: 47-58.e4.
- Yang H, Rudge DG, Koos JD, Vaidialingam B, Yang HJ, Pavletich NP. 2013. MTOR kinase structure, mechanism and regulation. *Nature* 497: 217–223.
- Yang X, Srivastava R, Howell SH, Bassham DC. 2016. Activation of autophagy by unfolded proteins during endoplasmic reticulum stress. *The Plant Journal* 85: 83–95.
- Ye K, Li H, Ding Y, Shi Y, Song C, Gong Z, Yang S. 2019. BRASSINOSTEROID-INSENSITIVE2 Negatively Regulates the Stability of Transcription Factor ICE1 in Response to Cold Stress in Arabidopsis. *The Plant Cell* 31: 2682–2696.
- Ye H, Liu S, Tang B, Chen J, Xie Z, Nolan TM, Jiang H, Guo H, Lin H-Y, Li L, et al. 2017. RD26 mediates crosstalk between drought and brassinosteroid signalling pathways. *Nature Communications* 8: 14573.

- Yin Y, Wang Z-Y, Mora-Garcia S, Li J, Yoshida S, Asami T, Chory J. 2002. BES1 Accumulates in the Nucleus in Response to Brassinosteroids to Regulate Gene Expression and Promote Stem Elongation. *Cell* 109: 181–191.
- **Youn J-H, Kim T-W. 2015**. Functional Insights of Plant GSK3-like Kinases: Multi-Taskers in Diverse Cellular Signal Transduction Pathways. *Molecular Plant* **8**: 552–565.
- Zhang Y, Song G, Lal NK, Nagalakshmi U, Li Y, Zheng W, Huang P, Branon TC, Ting AY, Walley JW, et al. 2019. TurbolD-based proximity labeling reveals that UBR7 is a regulator of N NLR immune receptor-mediated immunity. *Nature Communications* 10: 3252.
- Zhang D, Tan W, Yang F, Han Q, Deng X, Guo H, Liu B, Yin Y, Lin H. 2021. A BIN2-GLK1 Signaling Module Integrates Brassinosteroid and Light Signaling to Repress Chloroplast Development in the Dark. *Developmental Cell* 56: 310-324.e7.
- Zhang Z, Zhu J-Y, Roh J, Marchive C, Kim S-K, Meyer C, Sun Y, Wang W, Wang Z-Y. 2016. TOR Signaling Promotes Accumulation of BZR1 to Balance Growth with Carbon Availability in Arabidopsis. *Current Biology* 26: 1854–1860.
- Zhu J-Y, Li Y, Cao D-M, Yang H, Oh E, Bi Y, Zhu S, Wang Z-Y. 2017. The F-box Protein KIB1 Mediates Brassinosteroid-Induced Inactivation and Degradation of GSK3-like Kinases in Arabidopsis. *Molecular Cell* 66: 648-657.e4.

Figure Legends

- **Figure 1. Experimental design, workflow, and data overview.** (a) Schematic representation of the multi-omics processing pipeline for *bin2* and *raptor1b* mutants. (b) number of total detected transcripts, proteins, phosphoproteins, or phosphosites. NA = Not Applicable. (c) Differentially expressed transcripts, proteins, and phosphorylated amino acids for each analyzed mutant compared to wildtype (WT).
- **Figure 2. Gene ontology analysis on datasets.** Selection of significant gene ontology (GO) biological processes among differential expressed transcripts (**a**), proteins (**b**), and phosphosites (**c**), on *bin2D* (filled squares), *bin2T* (filled circles), and *raptor1b* (filled triangles). For transcripts and protein expression, significant terms were selected from

both, up- and downregulated genes. For phosphosites, terms were selected from those differentially expressed in the directionality of the respective kinase mutant (i.e., upregulated in *bin2D*, or downregulated in *bin2T* or *raptor1b*)

Figure 3. Phosphoproteomic analysis on *bin2* mutants shows significant enrichment of BIN2 direct targets. (a) Volcano plot of phosphorylation sites from a Multiplexed Assay for Kinase Specificity (MAKS) on Arabidopsis leaf protein extracts incubated with recombinant GST or GST-BIN2. Significantly increased phosphosites are colored blue (q < 0.1). (b) De novo motif enrichment analysis showed high enrichment for the GSK3 motif on BIN2-related phosphoproteomic datasets. Motif score and FoldEnrich values are calculated by motifeR, while *p*-value was calculated using hypergeometric testing. (c) Venn diagrams show overlap between BIN2 direct targets (i.e., those upregulated in BIN2 MAKS) and phosphosites (upper) or phosphoproteins (lower) upregulated in *bin2D* (left) or downregulated in *bin2T* (right) mutants. Numbers below each Venn diagram represent the overlapping percent for that mutant (purple = *bin2D*, orange = *bin2T*). Phosphosite overlaps were calculated using a 20 amino acid window, centered on the differentially regulated phosphosite (for details see methods section). Statistical significance was calculated using hypergeometric testing (*, P < 0.05; ***, P < 0.01).

Figure 4. Kinase signaling network. (a) A signaling network was inferred using phosphoproteomic data from *bin2D*, *bin2T*, and *raptor1b* mutants. Activated kinases are shown as named circles with their size representing the number of predicted targets (i.e., node outdegree). Target proteins are represented as small, purple circles. (b) De novo motif enrichment analysis among predicted direct targets (i.e., node first neighbors) for BIN2, MPK4, and MPK10 showed high enrichment for the GSK3 motif ([S/T]-X-X-X-[S/T]) and GSK3/MPK3 motif ([pS/pT]-P). Analysis on MPK6 predicted direct targets showed significant enrichment of MPK3/6 motif (P-X-[pS/pT]-P). Enrichment analysis was done on a 14 amino acids window, centered on target phosphosites. Motif enrichment significance was assessed through hypergeometric test.

Figure 5. Multi-dimensional integrative network. Kinase-signaling network (purple lines), abundance Gene Regulatory Network (GRN) (blue lines), and phosphosite GRN (green lines) were reconstructed for each mutant (i.e., *bin2D*, *bin2T*, and *raptor1b*) using transcriptomic, proteomic and phosphoproteomic information and merged into an integrative network (see methods section).

Figure 6. Phosphosite levels in *bin2D*, *bin2T*, and *raptor1b*. Scatterplot showing phosphosite intensity Log₂ fold-change (mutant/WT) for *raptor1b* on the x-axis and *bin2D* (a) or *bin2T* (b) on the y-axis. Red dots indicate phosphosites from selected candidate genes.

Figure 7. Hypocotyl response to BL treatment in selected mutant lines. (Upper) Average hypocotyl length on assayed mutants upon BL treatment. Bar plot showing average (n=24) hypocotyl length on mock (blue bars) or BL (green bars). Wild-type hypocotyl measurement in figure is the average across all experiments and is used only as visual reference. Error bars show standard error. (Lower) Heatmap showing hypocotyl length response to BL treatment. Values shown are the Log₂ fold change in hypocotyl length (BL/Mock); n=24. *, indicates P < 0.1 was observed in each of two independent experiments using a generalized linear model regression (Supporting Information Dataset S13a).

Figure 8. Autophagy levels on selected mutants. (a) Percentage of protoplast with high autophagy activity under normal conditions (basal autophagy, blue bars) and upon sucrose starvation (orange bars). (b) Heatmap showing fold-change in protoplasts with active autophagy between mutants and wildtype (WT) protoplasts. (Upper) Basal autophagy (mutant/WT) Log₂ fold-change. *, $P \le 0.05$, two-sample t-test. (Lower) Mutant autophagy response to sucrose starvation (starvation/mock) versus WT response to sucrose starvation (starvation/mock) versus WT response to sucrose starvation (starvation/mock). Values are Log₂ fold-change. *, $P \le 0.05$, generalized linear model. For all measurements, one-hundred protoplast were assessed in triplicate. Error bars show standard error. (\doteqdot) Cells from these genotypes did not survive sucrose starvation.

Figure 9. Proposed model of interaction for significant genes. Genes with significant response to brassinolide (BL) or altered autophagy levels are organized into groups

according to their mutants' phenotype. Solid, blunt-ended, lines represent the possibility of negative regulation whereas solid arrows are possible positive regulation. Dashed arrows depict possible upstream regulation of Target of Rapamycin Complex (TORC).

Supporting Information

Figure S1. Differential expression analysis

Figure S2. Workflow of signaling network reconstruction.

Figure S3. BES1 western blot.

Figure S4. S6K1/2 western blot.

Methods S1. Protein extraction for global proteome and phosphoproteome profiling

Methods S2. LC-MS/MS

Dataset S1: Mutant lines used for this study

Dataset S2: Curated list of Arabidopsis TFs and other TRs

Dataset S3: Transcriptomic, proteomic, and phosphoproteomic datasets

Dataset S4: GO analysis for bin2D, bin2T, and raptor1b DE transcripts

Dataset S5: GO analysis for bin2D, bin2T, and raptor1b DE proteins

Dataset S6: GO analysis for bin2D, bin2T, and raptor1b differentially phosphorylated proteins

Dataset S7: Motif enrichment analysis on BIN2 maks and bin2 mutants

Dataset S8: BIN2 direct targets (BIN2 MAKS) present in bin2D and bin2T phosphoproteome

Dataset S9: Activation loop coordinates for Arabidopsis thaliana kinases and list of kinases with activation state being modified in bin2D/WT, bin2TWT, or raptor1b/WT

Dataset S10: Kinase signaling network

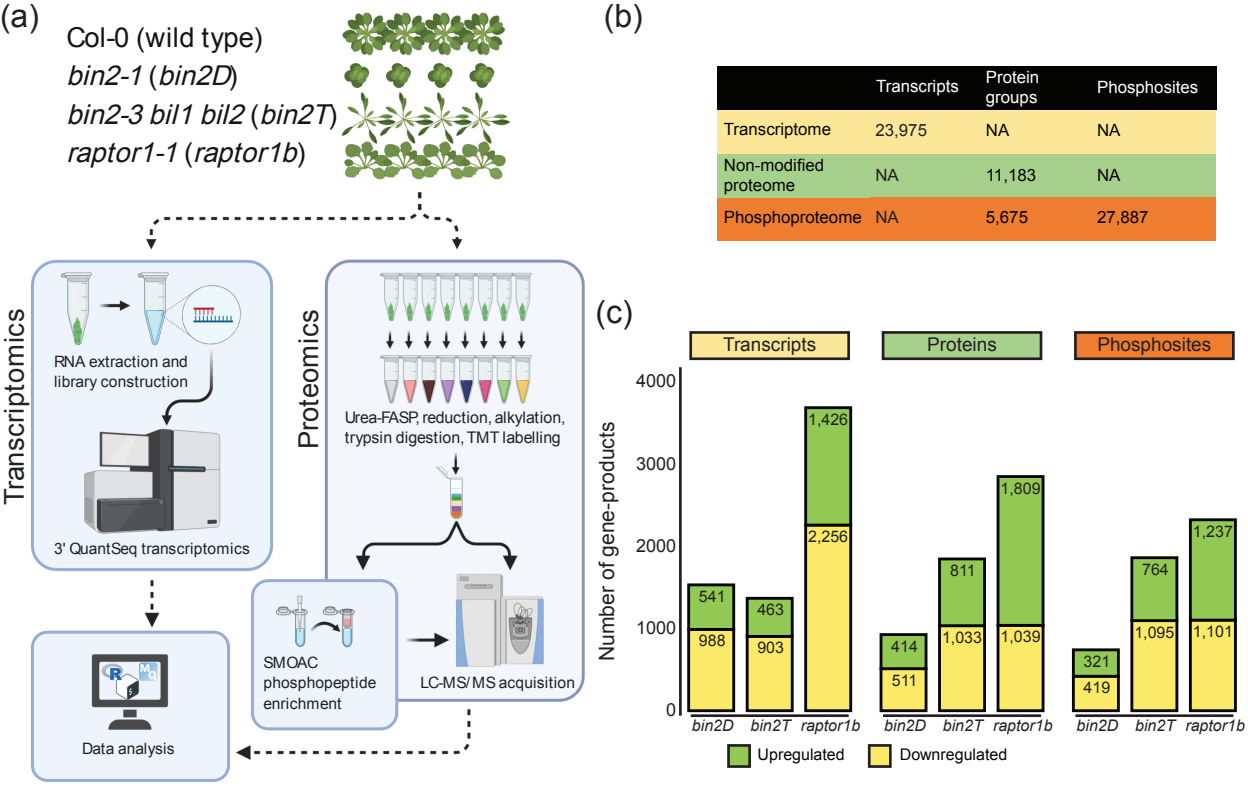
Dataset S11: Motif enrichment analysis on BIN2 and MAPKs targets predicted by signaling network

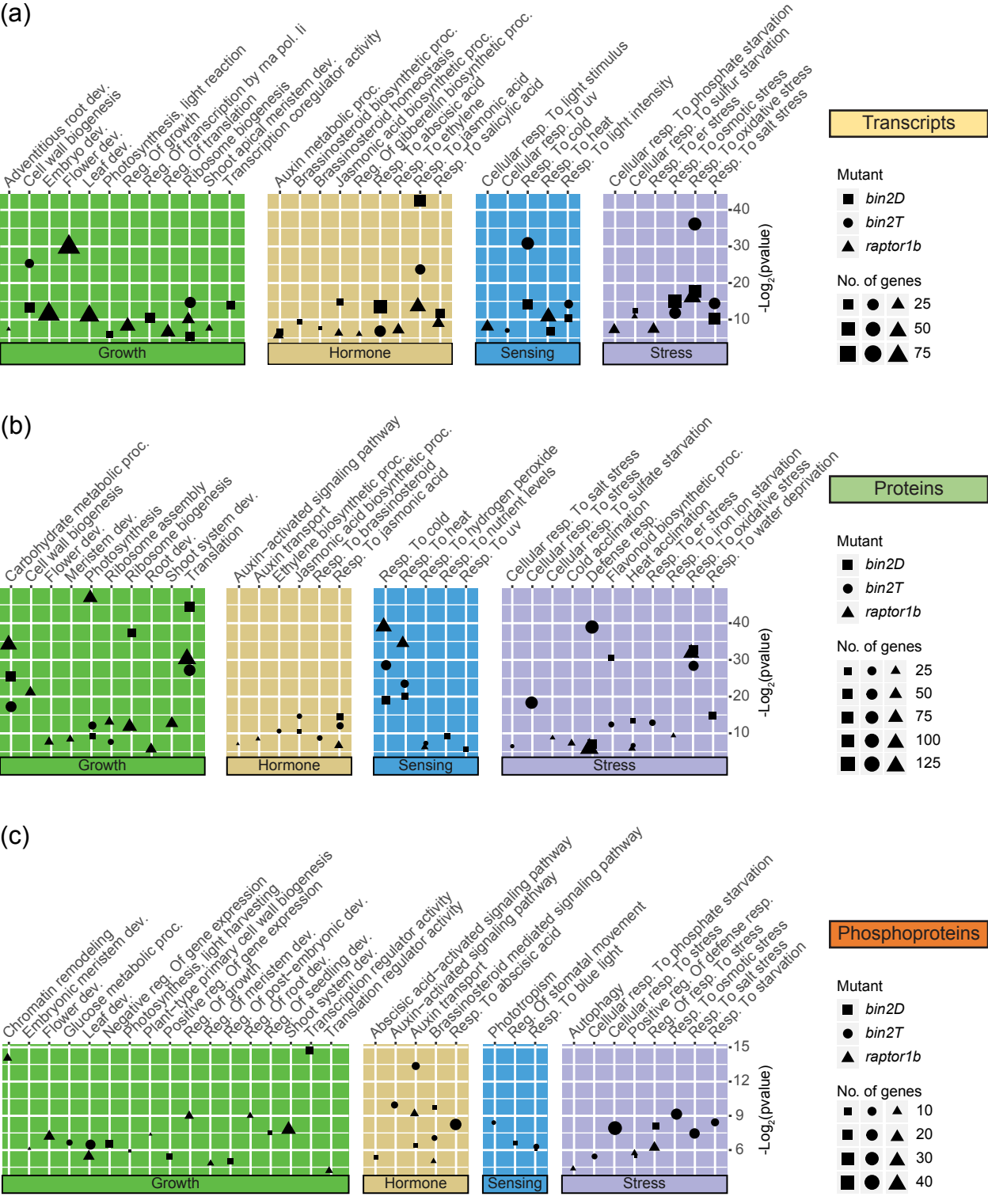
Dataset S12: Integrative network

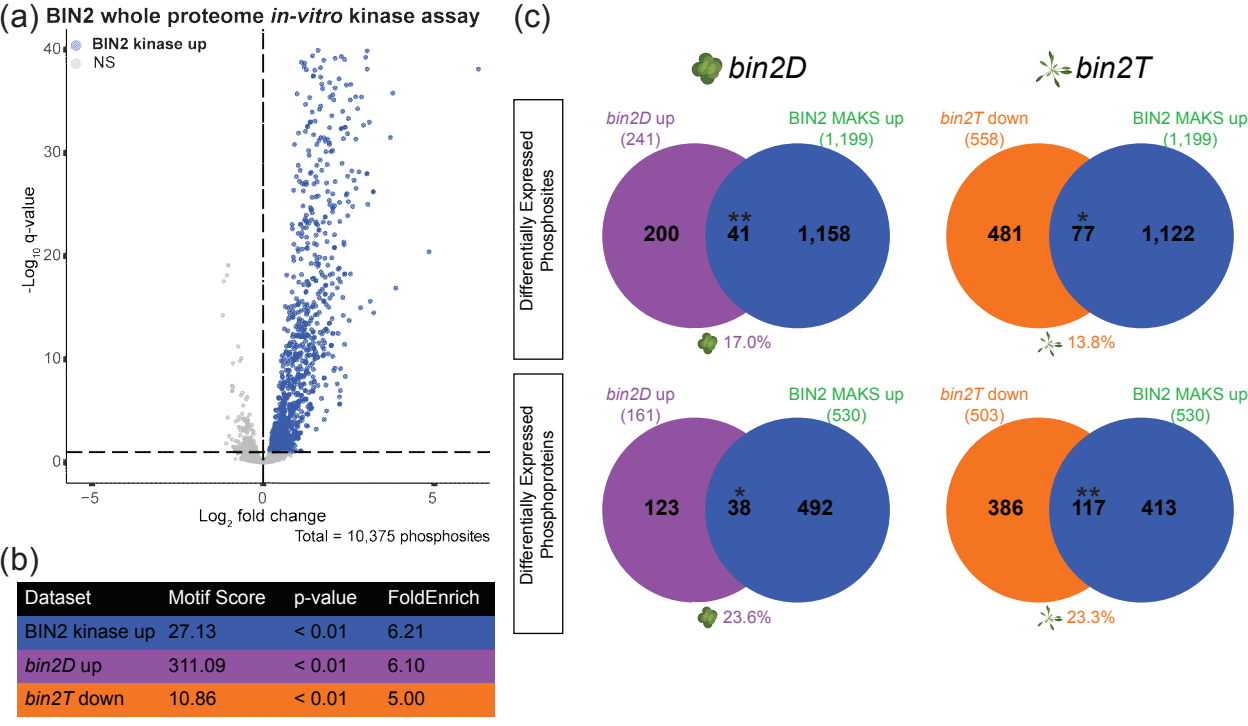
Dataset S13: BR and autophagy response phenotype on mutants from selected candidate genes

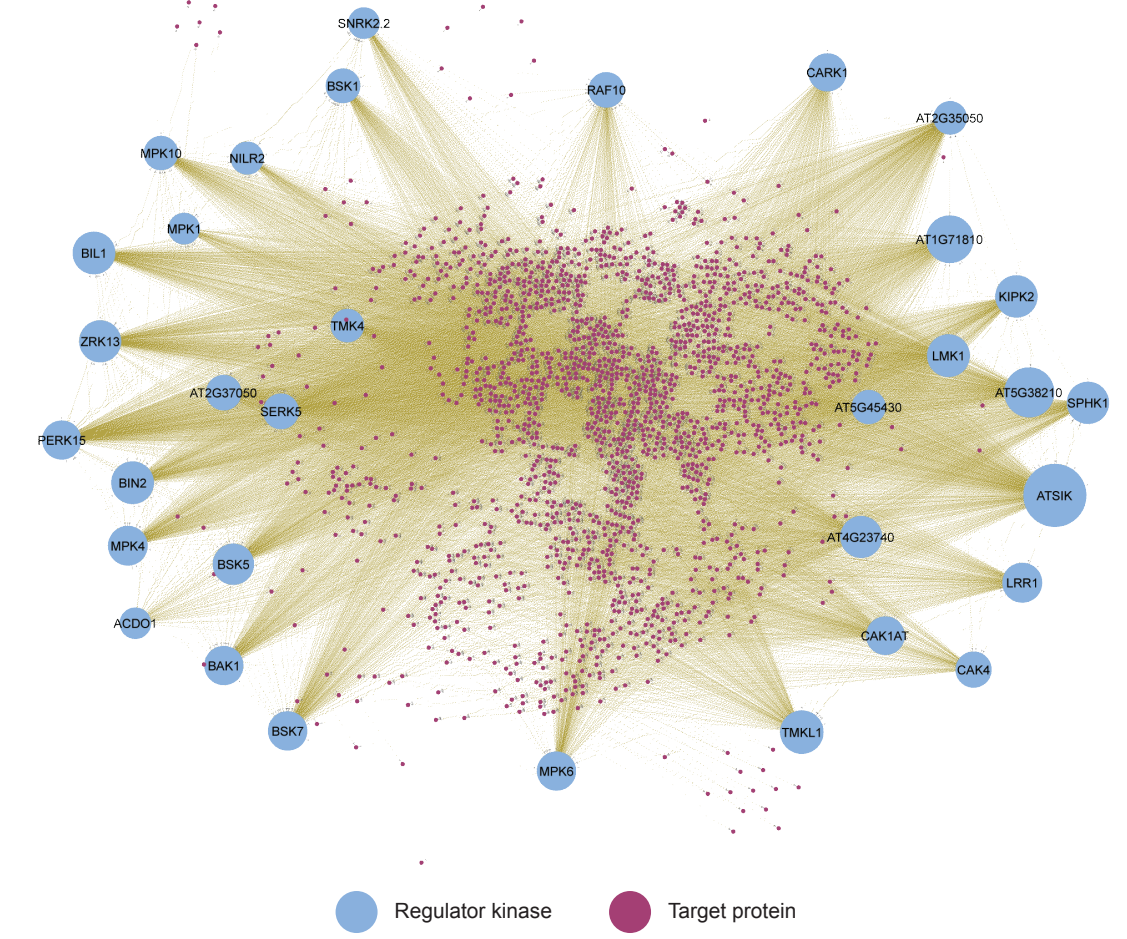
Table 1. Top ranked Arabidopsis thaliana regulator and target genes co-regulated by BIN2 and RAPTOR1B.

Gene ID	Gene Symbol	Outdegree	Indegree	IVI score	Node type	Mutant	Network
AT3G48360	BT2	1024	63	66.51	TF	CoReg	GRN
AT3G02830	ZFN1	1414	37	62.48	TF	CoReg	GRN; KS
AT2G13800	SERK5	825	36	58.79	Kinase	CoReg	GRN; KS
AT1G42990	BZIP60	911	84	56.04	TF	CoReg	GRN
AT4G23810	WRKY53	1010	87	54.60	TF	CoReg	GRN
AT1G15340	MBD10	857	99	54.06	TF	CoReg	GRN; KS
AT5G22380	NAC090	854	83	53.73	TF	CoReg	GRN
AT2G17040	NAC036	897	87	48.92	TF	CoReg	GRN
AT5G07100	WRKY26	554	70	44.24	TF	CoReg	GRN
AT3G48430	REF6	907	78	43.79	TF	CoReg	GRN; KS
AT2G35050	AT2G35050	684	50	43.18	Kinase	CoReg	GRN; KS
AT4G20400	JMJ14	946	63	42.14	TF	CoReg	GRN; KS
AT5G59010	BSK5	687	56	39.85	Kinase	CoReg	GRN; KS
AT4G12610	RAP74	758	69	38.98	TF	CoReg	GRN; KS
AT3G02380	COL2	772	78	37.18	TF	CoReg	GRN
AT1G71692	AGL12	917	12	37.17	TF	CoReg	GRN
AT5G18620	CHR17	785	68	37.04	TF	CoReg	GRN
AT2G36350	KIPK2	710	53	36.47	Kinase	CoReg	GRN; KS
AT4G34290	AT4G34290	634	43	35.10	TF	CoReg	GRN
AT4G35570	HMGB5	813	7	32.75	TF	CoReg	GRN
AT5G46710	AT5G46710	618	84	30.60	TF	CoReg	GRN
AT4G23740	AT4G23740	594	55	29.82	Kinase	CoReg	GRN; KS
AT5G58140	PHOT2	0	92	2.281	Target	CoReg	GRN; KS
AT1G72150	PATL1	0	84	2.160	Target	CoReg	GRN; KS
AT5G16880	TOL1	0	82	2.133	Target	CoReg	GRN; KS
AT4G39680	AT4G39680	0	93	2.104	Target	CoReg	GRN; KS
AT2G19910	RDR3	0	93	2.029	Target	CoReg	GRN
AT5G26860	LON1	0	74	2.022	Target	CoReg	GRN; KS
AT4G31430	AT4G31430	0	69	1.990	Target	CoReg	GRN; KS
AT4G02510	TOC159	0	81	1.988	Target	CoReg	GRN; KS
AT3G03960	ССТ8	0	59	1.986	Target	CoReg	GRN; KS
AT1G22530	PATL2	0	66	1.984	Target	CoReg	GRN; KS
AT1G62390	Phox2	0	67	1.984	Target	CoReg	GRN; KS
AT3G21060	RBL	0	72	1.979	Target	CoReg	GRN; KS
AT3G25130	AT3G25130	0	78	1.976	Target	CoReg	GRN









(a)

(b)

	- regulator runaco		ranger protein
Nodes	Regulator kinases	Target proteins	Target phosphosites
4,138	33	1,853	2,284

Subnetwork	Motif	Known kinase	motifeR Score	p-value	Fold enrichment
BIN2	[S/T]-X-X-X-[S/T]	GSK3	5.53	< 0.01	1.72
BIN2	[pS/pT]-P	GSK3/MPK	317.09	< 0.01	10.94
MPK4	[S/T]-X-X-X-[S/T]	GSK3	6.04	< 0.01	1.85
MPK4	[pS/pT]-P	GSK3/MPK	316.99	< 0.01	10.90
MPK6	P-x-[pS/pT]-P	MPK3/6	314.00	< 0.01	7.70
MPK10	[S/T]-X-X-X-[S/T]	GSK3	6.33	< 0.01	2.00
MPK10	[pS/pT]-P	GSK3/MPK	311.33	< 0.01	7.42

